



**HAL**  
open science

## A new view of the underside of Arctic sea ice

P Wadhams, Jp Wilkinson, Sd Mcphail

► **To cite this version:**

P Wadhams, Jp Wilkinson, Sd Mcphail. A new view of the underside of Arctic sea ice. *Geophysical Research Letters*, 2006, 33 (4), 10.1029/2005GL025131 . hal-03494192

**HAL Id: hal-03494192**

**<https://hal.science/hal-03494192>**

Submitted on 19 Dec 2021

**HAL** is a multi-disciplinary open access archive for the deposit and dissemination of scientific research documents, whether they are published or not. The documents may come from teaching and research institutions in France or abroad, or from public or private research centers.

L'archive ouverte pluridisciplinaire **HAL**, est destinée au dépôt et à la diffusion de documents scientifiques de niveau recherche, publiés ou non, émanant des établissements d'enseignement et de recherche français ou étrangers, des laboratoires publics ou privés.

Copyright

## A new view of the underside of Arctic sea ice

P. Wadhams,<sup>1,2</sup> J. P. Wilkinson,<sup>3</sup> and S. D. McPhail<sup>4</sup>

Received 4 November 2005; revised 5 January 2006; accepted 11 January 2006; published 17 February 2006.

[1] The Autosub-II autonomous underwater vehicle (AUV), operating off NE Greenland in August 2004, obtained the first successful swath sonar measurements under sea ice, showing in unprecedented detail the three-dimensional nature of the under-ice surface. The vehicle, operated from RRS *James Clark Ross*, obtained more than 450 track-km of under-ice multibeam data. We show imagery from first- and multiyear ice, including young ridges, old hummocks and undeformed melting ice. In addition, we show how the combination of other on-board sensors enabled the vehicle to obtain detailed information about seabed topography, water structure and current fields in an exploratory mode within a region which is seldom visited because of difficult year-round ice conditions. This included identification of a new current regime in the Norske Trough. **Citation:** Wadhams, P., J. P. Wilkinson, and S. D. McPhail (2006), A new view of the underside of Arctic sea ice, *Geophys. Res. Lett.*, 33, L04501, doi:10.1029/2005GL025131.

### 1. Introduction

[2] In August 2004 the Autosub-II AUV was taken to NE Greenland (NEG) aboard RRS *James Clark Ross*, and carried out under-ice exploration of the continental shelf from 79°N northward, using an upward-looking Simrad EM2000 multibeam echo sounder for ice profiling as well as oceanographic sensors and downward ADCP. The wide shelf includes the Belgica and Ob' Banks (Figure 1), of which the Belgica Bank is locally shallow, containing small low-lying ice-push islands such as Tobias Island [Mohr and Forsberg, 2001]. It is separated from the Greenland coast by a system of connected troughs (Belgica, Norske, and Westwind) with outlets to south and north, while to the east lies Fram Strait with the cold southward-flowing East Greenland Current (EGC). Ice conditions over the bank-trough system are usually heavy. Ridged polar ice from the EGC grounds on Belgica Bank together with broken-out thin tabular icebergs from nearby Greenland glaciers such as the 79 Glacier and the Zachariae Isstrøm, where a major iceberg breakout was observed in 2003. The grounded masses are pinning points for a locally-grown fast ice sheet which extends across the Norske Trough to the Greenland coast, known as the Norske Øer Ice Barrier (NØIB) [Reeh *et al.*,

2001]. Breakup of NØIB was once rare, occurring about every 50 years [Higgins, 1989, 1991] but it disintegrated in the summers of 1997, 2002, 2003 and 2004; in early September 2003 no ice at all was left on the NEG shelf. North of the ice barrier lies a polynya near Ob' Bank known as the Northeast Water (NEW), lasting from May/June until September [Böhm *et al.*, 1997].

[3] After test missions under drifting ice (M361-2, Figure 1) a series of Autosub missions was despatched westward from the Belgica Bank fast ice edge toward the Greenland coast, passing first through shallow water north of the Northwind Shoal, then into the deeper Norske Trough, reaching close to the Greenland coast. The missions lasted up to 25 hours, covering 150 km of track. Data from M365 are reported here. While Autosub was under the ice the shipboard team ran lines of drilled holes at 5 m intervals along the axis of the vehicle's track near the ice edge and took ice cores.

[4] The ship moved northward to 80°17'N 13°01'W, to Westwind Trough and the area of the NEW Polynya. From the fast ice edge mission 366 was carried out (Figure 1), accompanied by drilling and coring. The ship then returned to her former fast ice edge position at 79°21'N, 13°52'W for further transects.

### 2. Ocean Currents and Bathymetry

[5] Figure 2 shows results from the 68 km outward track of M365 run at 40 m depth. Firstly, we see that the bathymetry of IBCAO (International Bathymetric Chart of the Arctic Ocean), itself updated in 2001 [Jakobsson *et al.*, 2000] (see also <http://www.ngdc.noaa.gov/mgg/bathymetry/arctic/arctic.html>) is deficient, showing deeper water over Belgica Bank and shallower water over Norske Trough than Autosub, with less detailed topography. Autosub shows Norske Trough to be at least 460 m deep near its western end, while IBCAO shows 200 m.

[6] Two exciting features of Figure 2 are the ice thickness distribution (represented by the low-resolution upward ADCP profile) and the nature of the ocean currents, shown by the upward and downward-looking ADCP record. The ice profile shows that the Belgica Bank shallows were covered with ridged ice, while the Norske Trough was covered by an undeformed, locally-grown fast ice sheet less than 2 m thick, with a second small area of ridging near Greenland.

[7] The ADCP data show the northward velocity component, normally detectable down to depths of 100–150 m (dependent on the concentration of scatterers in the water column). The red zone on the left of the Figure 2 shows that at 50–60 km penetration, and at water depths from the surface to 100 m, there is a strong northward current component of 0.2–0.25 m s<sup>-1</sup>, while at 35–45 km penetration, and at water depths of 100–120 m, there is a strong

<sup>1</sup>Department of Applied Mathematics and Theoretical Physics, University of Cambridge, Cambridge, UK.

<sup>2</sup>Formerly at Laboratoire d'Océanographie de Villefranche, Université Pierre et Marie Curie, Villefranche-sur-Mer, France.

<sup>3</sup>Scottish Association for Marine Science, Dunstaffnage Marine Laboratory, Dunbeg, UK.

<sup>4</sup>National Oceanography Centre, Southampton, UK.

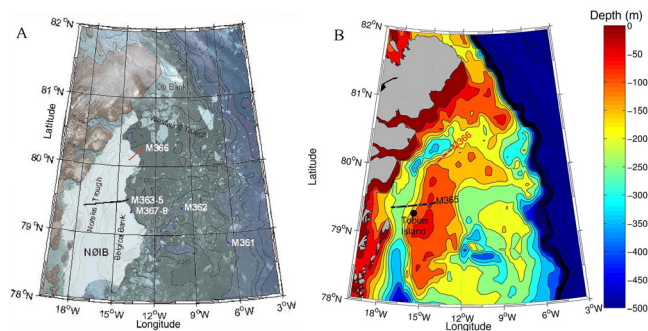


**Figure 1.** (a) MODIS visual image of ice extent on NE Greenland shelf, 12 August 2004. Bathymetric features mentioned in the text are shown, and the locations of Autosub-II missions (M361-2 were test missions in Fram Strait, M363-5 and M367-8 were launched from a single ice edge position on Belgica Bank, M366 was launched from Westwind Trough). (b) Bathymetry of the NE Greenland shelf, according to IBCAO. Tracks of missions M365 and M366 are shown.

southward component of  $0.15\text{--}0.25\text{ m s}^{-1}$ . The shelf circulation in this area was first described by *Bourke et al.* [1987] and refined by the IAPP [*Overland et al.*, 1995; *Hirche and Deming*, 1997]. They defined a northward-flowing Northeast Greenland Coastal Current (NGCC) within the trough system. *Schneider and Budéus* [1997] hypothesised that the NGCC keeps the NEW open since its burden of sea ice is held back by the NØIB. We can identify the northward current seen by Autosub with the NGCC but the southward current is a hitherto unrecognized counter-current. It may be a northward extension of a current found by *Budéus and Schneider* [1995] in Belgica Trough. The two current cores are less than 20 km apart and shear between them may generate enough scatterers to allow the deeper ADCP return seen in the region between the currents in Figure 2.

### 3. Multibeam Sonar Data

[8] Figure 3 shows some examples of the high quality of data derived from the multibeam sonar system. Each displayed image is a perspective view of the underside of ice, obtained at 40 m depth. The scenes are illuminated by a sun of elevation  $20^\circ$ . Alongside each image is a probability density function (pdf) of ice draft for the image region compared with a pdf for the entire mission. The crude ice draft profile of Figure 2 shows the different ice regimes, but the 3-D data enable us to see that the ice over Belgica Bank was not just heavily ridged but a combination of ridges and thick floes frozen into place by ice formed the previous winter.

[9] Figure 3a shows the deepest ridge encountered during M365, marked A in Figure 2. It is 33 m deep, and represents a formidable ice mass (the slice in the figure weighs about 200,000 tons). Since the individual ice blocks in ridges are quite small, the ridge itself is a relatively uniform triangle in cross-section, representing the angle of repose of a pile of buoyant ice. *Wadhams* [1978a] drew attention to this characteristic of ridges deeper than 30 m in an analysis of

submarine profiles. A lesser ridge is visible in the foreground. The undeformed ice on the nearside corner of the image is 1.75 m in draft (first-year) and between the two ridges is 4 m (multi-year); it is likely that the giant ridge, the smaller ridge and the intervening ice form part of an embedded floe that has drifted from the Arctic Ocean.

[10] Figure 3b is a  $100 \times 250\text{ m}$  image also from Belgica Bank. It shows an old multi-year ridged floe of thickness 3–5 m which is embedded in younger fast ice of draft 1.8 m. The older, thicker floe resembles floes seen in the marginal ice zone (MIZ) of Fram Strait, where large sheets of polar sea ice are fractured by wave action and turned into floes of typical diameter 100 m retaining fragments of their original pressure ridges. The edges of the floe are angular as would occur with a fracture which occurred just before embedding. The ridge which occupies half of the floe has maximum draft 11 m and contains separate ice blocks of typical diameters 5–20 m. Probably before embedding it was in a state of disintegration or melt; observations in the MIZ often show such floes shedding ice blocks from their underside under the impact of waves. The surrounding thinner ice is probably first-year ice despite its unusual thickness. The faint pattern of depressions in the underside occurs because of the presence on the upper surface of meltwater pools. These pools preferentially absorb incoming radiation, giving a heat flux which enhances bottom melt and generates a bottom depression which mirrors the pool's position on the top side [*Wadhams and Martin*, 1990; *Wadhams*, 2000]. Although the existence of such topographic features has been inferred from topside observations, and their general shape has been revealed by sidescan sonar imagery [*Wadhams*, 1988], the quantitative data shown here mark a significant advance in the understanding of ice bottom topography.

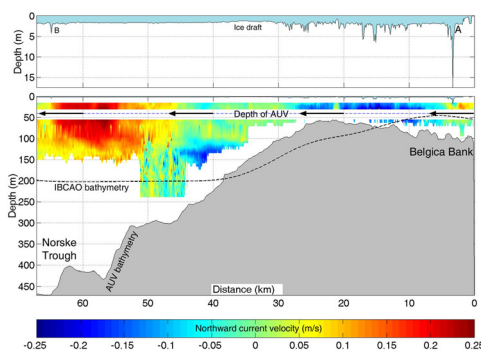
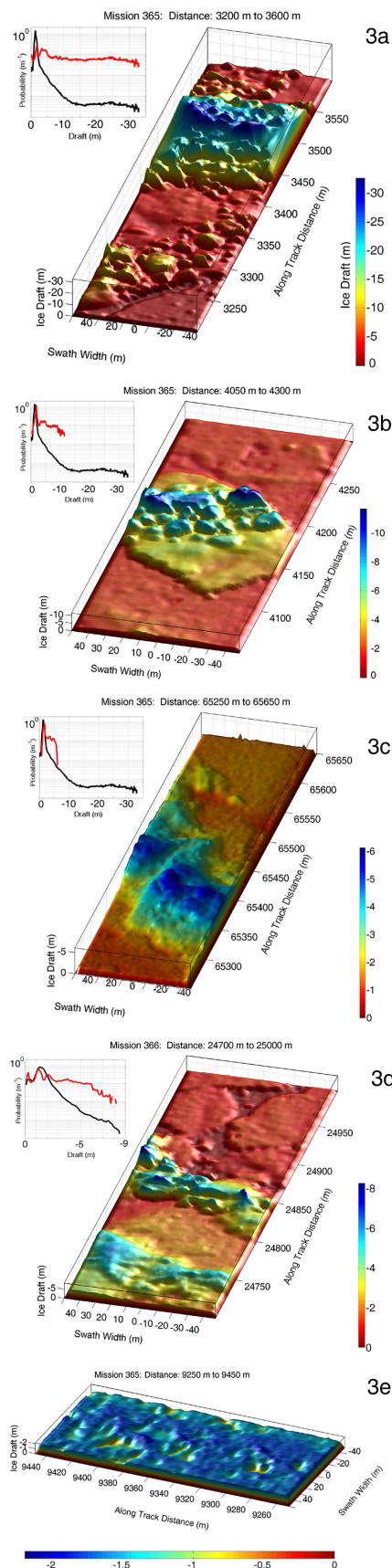


**Figure 2.** The outward track of mission 365, 21–22 August 2004, runs at 40 m depth. (top) Ice draft measured at crude resolution by upward-looking ADCP; A and B are ridges shown in Figure 3 whose depths are underestimated by the ADCP. Note smooth undeformed ice over Norske Trough. (bottom) The seabed topography measured by Autosub compared with the IBCAO bathymetry (dashed line). The coloured masses are N-S velocity components measured by the downward looking ADCP aboard Autosub. The red area is a strong northward current in the Trough, the Northeast Greenland Coastal Current (NGCC); the blue area is a hitherto unrecognised southward current on the western flank of Belgica Bank.



[11] Figure 3c is from the western limit of M365, near the coast of Greenland. It shows a pressure ridge of 6 m draft (B in Figure 2), the only ridge in this region after more than 30 km of undeformed fast ice. The ridge axis is oriented at  $45^\circ$  to the track of the AUV. The fast ice around the ridge has 1.7 m draft, while further to the east, across the trough and bank, it is only 1.0–1.3 m, indicating either that in this western part of Norske Trough, close to the continental influence of Greenland, the ice grows more rapidly, or that unbalanced isostasy in the ridge is affecting the draft of nearby ice.

[12] Figure 3d is an image from M366 in Westwind Trough (Figure 1), showing in the background well-rounded first-year floes (draft 1.2 m) glued together by very young ice (thickness 0.25 m), with a young (probably first-year) ridge in the centre of the image and an old worn-down hummock in the front. Between the two is a multi-year floe of thickness 1.85–2.25 m containing the hummock. The young ridge is narrower and more linear than that of Figure 3c and may be a shear ridge rather than a pressure ridge, formed by motion between the first-year ice and the older floe. The contrast between the sharpness of topography in the two ridges is dramatic, showing the effect of a number of years of ageing and partial melt in rounding off the blocky topography of the older ridge.

[13] Figure 3e is a typical example of a large undeformed multi-year floe which has developed a much deeper system of melt pool-associated depressions than the first-year ice of

**Figure 3.** Some examples of EM-2000 multibeam ice draft data in perspective views, as if illuminated by a sun of elevation  $20^\circ$ . Data points fill  $2\text{ m} \times 2\text{ m}$  grid. No vertical exaggeration unless otherwise stated. Each image is accompanied by a probability density function (pdf) of ice draft compared to the pdf of the mission as a whole (lin-log scale, 5 cm bins). (a) Deep 33 m ridge on Belgica Bank, marked A in Figure 2, with shallower ridge in foreground, both surrounded by undeformed ice. (b) Thick multi-year ridged floe of draft 3–5 m, with linear edges suggesting production from fracture of larger ice sheet, embedded in undeformed fast ice of draft 1.8 m. Fast ice shows pattern of depressions due to mirroring of surface melt pools. Thicker ice contains pressure ridge of maximum draft 11 m which has partly disintegrated into individual ice blocks of diameter 5–20 m. Evidence is that thicker floe came from MIZ. (c) Pressure ridge B in Figure 2, from western side of Norske Trough. Maximum draft 6.0 m. Smooth undeformed ice has peaks at 1.7 m and 1.3 m. Vertical exaggeration 1.75:1. (d) Image from M366 showing in background first-year floes of 1.2 m draft with rounded edges embedded in young ice of 0.25 m draft. In centre is young linear ridge, possibly shear ridge formed between the first-year ice and thicker floe in foreground. Foreground floe is multi-year ice of 1.85–2.25 m draft and in front a worn-down multi-year hummock. Vertical exaggeration 1.25:1. (e) Multi-year undeformed floe which has developed deep craters in underside to match deep surface meltwater pools. Modal draft is 1.7 m, with maximum of 2.2 m and with some craters as thin as 0.5 m. Vertical exaggeration 4:1.

Figure 3b. The contrast between very shallow pools (Figure 3b) and canyon-like craters is because each year the refrozen melt pools from the year before reopen and deepen, causing increased compensating melt on the underside. This image is vertically enhanced to 4:1 to show the crater-like nature of the features. We infer that the floe was multiyear despite a modal draft of only 1.7 m because it lay close to our validation line, where the modal draft was also 1.7 m and where the thickness-averaged salinity of the ice cores was only 0.96 PSU, typical of multiyear ice.

[14] The accompanying pdfs are of great interest. The advantage of having 111 beams is that statistically valid pdfs can be obtained over much shorter distances than the 50 km commonly employed for single-beam upward sonar. The pdfs yield wholly new information about ice draft distribution. It is already known from long upward sonar profiles that the pdf has a tail with a negative exponential form [Wadhams, 2000] but now we see that this is created by the superposition of a series of top hat functions (e.g., Figures 3a, 3b, and 3c), each due to a single ridge, which are flat as far as an ultimate drop-off depth, as would be expected from a basically triangular geometry. The overall pdf of M365 approaches a negative exponential from 3–10 m draft but then flattens out as the only contribution to deeper ice comes from a single ridge.

[15] These results show the advantages of high-resolution quantitative 3-D images, as compared to a single-beam profile or the qualitative shadow pattern of sidescan. Previous reported AUV operations under ice comprise an Autosub cruise under Antarctic sea ice with a single beam sonar [Brierley *et al.*, 2002]; and an operation off East Greenland by the Danish Maridan AUV which yielded sidescan sonar imagery of the ice underside [Wadhams *et al.*, 2004]. Sidescan sonar imagery of sea ice has also been obtained from military submarines [Wadhams, 1978b, 1988]; otherwise to date all reported under-ice sonar profiles have been one-dimensional.

#### 4. Conclusions

[16] Autosub operated very successfully under Arctic sea ice, obtaining 458 km of high quality multibeam sonar and oceanographic data. It undertook avoidance manoeuvres for obstacles, and an acoustic homing system allowed the vehicle to be returned with confidence to an area covered with loose moving pack ice. The combination of an unmanned under-ice vehicle and a multibeam sonar gives, literally, a new dimension to under-ice studies, and is important for work on the role of ice in climate change. This is now especially important since the availability of military submarines for Arctic under-ice research has diminished, while new satellite altimetry methods require validation by high-resolution ice draft profiling before acceptance of thickness values inferred from the observed freeboards.

#### Appendix A: The Multibeam Sonar

[17] The Simrad EM2000 uses the so-called “Mills Cross” configuration, whereby the along-track resolution

is provided by the transmitter beam pattern, and the across-track resolution is provided by the receiver array. The system transmits a 200  $\mu$ s sonar pulse at 200 kHz every 1.6 s. The transmit beam is 1.5° wide in the along-track direction and insonifies a segment of total angle 120° across track (60° each side). The receive array synthesises the across-track beams with a resolution of 2.5°. The ice draft measurements are calculated from the ranges, the beam angles, the depth of the AUV and the roll, pitch and heading of the AUV. Hence the resolution and accuracy of the ice draft depend upon the depth of the AUV below the ice. At 40 m, the along-track resolution is 1 to 2 m, and across-track is about 1.8 m. Ice draft accuracy depends upon whether in-situ calibrations of zero ice thickness (e.g., leads) can be made during the survey. Where this is possible, then the single measurement accuracy is limited by system quantisation and noise, and systematic biases. Post-processing can minimise systematic differences in ice draft measurements across the track due to ray bending and differing grazing angles. We estimate overall average, ice draft uncertainty as 5 cm (to one standard deviation).

[18] **Acknowledgments.** We thank the UK NERC for support under the Autosub-under-Ice program grant no. NER/T/S/2000/00985, and the captain and crew of RRS *James Clark Ross*. We are grateful to the AUV technical team on board (P. Stevenson, J. Perrett, K. Rutherford, M. Squires, A. Webb, D. White) for successful operation of the vehicle; to Povl Abrahamsen (BAS) and Kate Stanfield (National Oceanography Centre) for ADCP software; and to Arthur Kaletsky (DAMTP), Nick Hughes (SAMS, Oban) and Guy Williams (ACE, Hobart) for assistance in data processing. Additional support was provided by the European Commission under the SITHOS project.

#### References

- Böhm, E., T. S. Hopkins, and P. J. Minnett (1997), Passive microwave observations of the Northeast Water Polynya: 1978–1994, *J. Mar. Syst.*, *10*, 85–94.
- Bourke, R. H., J. L. Newton, R. G. Paquette, and M. D. Tunnicliffe (1987), Circulation and water masses of the East Greenland Shelf, *J. Geophys. Res.*, *92*, 6729–6740.
- Brierley, A. S., N. W. Millard, S. D. McPhail, P. Stevenson, M. Pebody, J. Perrett, M. Squires, and G. Griffiths (2002), Antarctic krill under sea ice: Elevated abundance in a narrow band just south of ice edge, *Science*, *295*, 1890–1892.
- Budéus, G., and W. Schneider (1995), On the hydrography of the Northeast Water Polynya, *J. Geophys. Res.*, *100*, 4287–4299.
- Higgins, A. K. (1989), Mammals of central north Greenland, *Polar Rec.*, *25*, 207–212.
- Higgins, A. K. (1991), North Greenland glacier velocities and calf ice production, *Polarforschung*, *60*, 1–23.
- Hirche, H.-J., and J. W. Deming (Eds.) (1997), Northeast Water Polynya symposium, *J. Mar. Syst.*, *10*, 524 pp.
- Jakobsson, M., N. Cherkis, J. Woodward, R. Macnab, and B. Coakley (2000), New grid of Arctic bathymetry aids scientists and mapmakers, *Eos Trans. AGU*, *81*, 89, 93, 96.
- Mohr, J. J., and R. Forsberg (2001), Searching for new islands in sea ice, *Nature*, *416*, doi: 10.1038/416035a.
- Overland, J. E., T. B. Curtin, and W. O. Smith Jr. (Eds.) (1995), Leads and Polynyas, *J. Geophys. Res.*, *100*, 4267–4843.
- Reeh, N. C., H. H. Thomsen, A. K. Higgins, and A. Weidick (2001), Sea ice and the stability of north and northeast Greenland floating glaciers, *Ann. Glaciol.*, *33*, 474–480.
- Schneider, W., and G. Budéus (1997), Summary of the Northeast Water Polynya formation and development (Greenland Sea), *J. Mar. Syst.*, *10*, 107–122.
- Wadhams, P. (1978a), Characteristics of deep pressure ridges in the Arctic Ocean, in *POAC 77: 4th International Conference on Port*

- and Ocean Engineering Under Arctic Conditions*, vol. 1, Mem. Univ. of Newfoundland, St. John's, Newfoundland, Canada.
- Wadhams, P. (1978b), Sidescan sonar imagery of sea ice in the Arctic Ocean, *Can. J. Remote Sens.*, *4*, 161–173.
- Wadhams, P. (1988), The underside of Arctic sea ice imaged by sidescan sonar, *Nature*, *333*, 161–164.
- Wadhams, P. (2000), *Ice in the Ocean*, Taylor and Francis, Philadelphia, Pa.
- Wadhams, P., and S. Martin (1990), Processes determining the bottom topography of multiyear Arctic sea ice, in *Sea Ice Properties and Processes*, *CRREL Monogr.*, 90-1, edited by S. F. Ackley and W. F. Weeks, pp. 136–141, U. S. Army Cold Reg. Res. and Eng. Lab., Hanover, N. H.
- Wadhams, P., J. P. Wilkinson, and A. Kaletzky (2004), Sidescan sonar imagery of the winter marginal ice zone obtained from an AUV, *J. At. Oceanic Technol.*, *21*, 1462–1470.
- 
- S. D. McPhail, National Oceanography Centre, Empress Dock, Southampton SO14 3ZH, UK.
- P. Wadhams, Department of Applied Mathematics and Theoretical Physics, University of Cambridge, Wilberforce Road, Cambridge CB3 0WA, UK. (p.wadhams@damtp.cam.ac.uk)
- J. P. Wilkinson, Scottish Association for Marine Science, Dunstaffnage Marine Laboratory, Dunbeg PA37 1QA, UK.